BIOCHEMISTRY
including biophysical chemistry & molecular biology

Article

pubs.acs.org/biochemistry

Improving upon Nature: Active Site Remodeling Produces Highly Efficient Aldolase Activity toward Hydrophobic Electrophilic Substrates

Manoj Cheriyan,[†] Eric J. Toone,[‡,§] and Carol A. Fierke*[,†,∥]

[†]Department of Chemistry, University of Michigan, Box 1055, Ann Arbor, Michigan 48109, United States
[‡]Department of Chemistry, Duke University, Box 90317, Durham, North Carolina 27708, United States
[§]Department of Biochemistry, Duke University Medical Center, Durham, North Carolina 27710, United States
[∥]Department of Biological Chemistry, University of Michigan, Ann Arbor, Michigan 48109, United States

Supporting Information

ABSTRACT: The substrate specificity of enzymes is frequently narrow and constrained by multiple interactions, limiting the use of natural enzymes in biocatalytic applications. Aldolases have important synthetic applications, but the usefulness of these enzymes is hampered by their narrow reactivity profile with unnatural substrates. To explore the determinants of substrate selectivity and alter the specificity of *Escherichia coli* 2-keto-3-deoxy-6-phosphogluconate (KDPG) aldolase, we employed structure-based mutagenesis coupled with library screening of mutant enzymes localized to the bacterial periplasm. We identified two active site mutations (T161S and S184L) that work additively to enhance the substrate specificity of this aldolase to include catalysis of retro-aldol cleavage of (4*S*)-2-keto-4-hydroxy-4-(2′-pyridyl)butyrate (*S*-KHPB). These mutations improve the value of $k_{cat}/K_M^{S\text{-KHPB}}$ by >450-fold, resulting in a catalytic efficiency that is comparable to that of the wild-type enzyme with the natural substrate while retaining high stereoselectivity. Moreover, the value of $k_{cat}^{S\text{-KHPB}}$ for this mutant enzyme, a parameter critical for biocatalytic applications, is 3-fold higher than the maximal value achieved by the natural aldolase with any substrate. This mutant also possesses high catalytic efficiency for the retro-aldol cleavage of the natural substrate, KDPG, and a >50-fold improved activity for cleavage of 2-keto-4-hydroxy-octonoate, a nonfunctionalized hydrophobic analogue. These data suggest a substrate binding mode that illuminates the origin of facial selectivity in aldol addition reactions catalyzed by KDPG and 2-keto-3-deoxy-6-phosphogalactonate aldolases. Furthermore, targeting mutations to the active site provides a marked improvement in substrate selectivity, demonstrating that structure-guided active site mutagenesis combined with selection techniques can efficiently identify proteins with characteristics that compare favorably to those of naturally occurring enzymes.

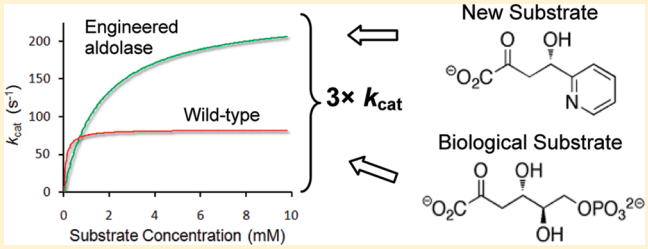

Aldolases make up a class of structurally and mechanistically diverse enzymes that catalyze reversible aldol addition reactions and have demonstrated utility as biocatalysts.[1−3] This class of enzymes has long been used for the synthesis of carbohydrates because of their rapid catalysis, high stereospecificity, and regioselectivity. Four classes of aldolases have been described on the basis of the identity of the preferred nucleophilic substrate (Table S1 of the Supporting Information). The aldolases most widely used for biocatalysis prefer dihydroxyacetone phosphate (DHAP) as the nucleophilic substrate (DHAP aldolases). Although enzymes that preferentially generate each of the four diasteromeric products at the bond-forming carbon centers have been isolated, these aldolases have limited synthetic usefulness because of difficulties associated with the absolute requirement for DHAP as the nucleophilic substrate, a species that is both difficult to synthesize and unstable, making it a poor choice for large-scale synthetic applications.[4,5] For this reason, a number of researchers have worked on engineering DHAP aldolases or identifying alternative aldolases that do not require phosphorylated electrophiles.[6−9]

The pyruvate aldolases use pyruvate as the native nucleophilic substrate, an advantage for synthetic applications because it is both inexpensive and stable under most conditions. Additionally, the 2-keto-4-hydroxybutyrate products that result from pyruvate aldolase-catalyzed aldol addition include all four commonly found oxidation states of carbon, giving the synthetic chemist differential handles for selective transformation in the subsequent steps. Figure 1 illustrates the range of transformations available from the product of pyruvate aldol condensation. We have focused our efforts on optimizing the pyruvate aldolase, 2-keto-3-deoxy-6-phosphogluconate (KDPG) aldolase, for use as a biosynthetic catalyst. This enzyme is attractive as a

Received: December 20, 2011
Revised: January 31, 2012
Published: February 1, 2012

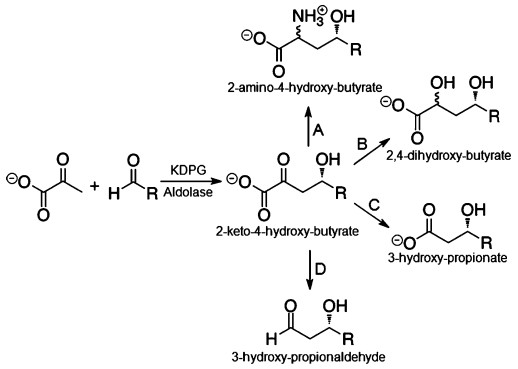

Figure 1. Pyruvate aldolase-catalyzed stereospecific aldol reaction and synthetic elaborations of the 2-keto-4-hydroxybutyrate product:[48] (A) reductive amination, (B) reduction, (C) oxidative decarboxylation, and (D) nonoxidative decarboxylation.

biocatalyst because it possesses a broad pH optimum, high tolerance of organic cosolvents, and high stereoselectivity and is easily overexpressed and purified.[10]

The majority of aldolases studied to date catalyze transformations of carbohydrates, primarily catalyzing the retro-aldol cleavage of carbohydrates to three-carbon fragments.[4] BphI and HpaI aldolases are class II (metal-dependent) aldolases that catalyze reactions with unfunctionalized aliphatic aldehydes.[11,12] Similarly, KDPG aldolase, the final enzyme in the Entner–Doudoroff pathway, is a class I aldolase that catalyzes the reversible aldol cleavage of the phosphorylated sugar acid, KDPG, to pyruvate and glyceraldehyde 3-phosphate (Scheme 1). In the synthetic direction, efficient catalysis is generally restricted to the reaction of pyruvate with a phosphorylated

Scheme 1. Catalytic Mechanism[a] of *Escherichia coli* KDPG Aldolase[29,30]

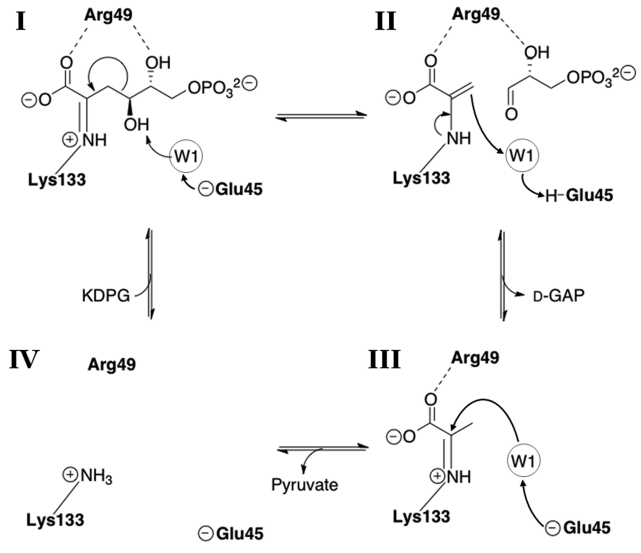

[a]The substrate is bound as a Schiff base adduct with Lys133 (**I**), and water W1 arises from the keto group that is displaced by Schiff base formation.[30] Glu45 catalyzes the removal of a proton from the C4 hydroxyl of KDPG. This proton transfer is mediated by W1. The C3–C4 bond is broken with the Schiff base stabilizing the formation of a carbanion at C4 to form D-glyceraldehyde 3-phosphate and a pyruvyl-enamine (**II**). The pyruvyl-enamine is protonated by the acidic form of Glu45 via W1 to form a Schiff base (**III**). Finally, the pyruvyl-Schiff base is hydrolyzed, resulting in the free enzyme (**IV**).

polyhydroxy aldehyde,[10] limiting the synthetic utility of the natural enzyme. A number of researchers have attempted to expand the substrate profile of KDPG[13−15] and the structurally and mechanistically related KDPGal[16] aldolases by directed evolution with modest success. Pyruvate aldolases that catalyze aldol reactions with unfunctionalized aliphatic and aromatic aldehydes remain a desirable target for biocatalytic applications.

Here we use structure-guided mutagenesis to prepare KDPG aldolase mutants that increase the catalytic efficiency with hydrophobic aldehydes up to 450-fold while maintaining exquisite stereoselectivity. The high catalytic efficiency of these engineered enzymes with aliphatic aldehydes may aid future efforts in the chemoenzymatic synthesis of antimicrobial compounds such as syringomycin E[17] and lyngbyaballin A[18](Figure S1 of the Supporting Information). Furthermore, the ability to catalyze the aldol addition of pyruvate and pyridine carboxaldehydes is useful for the synthesis of analogues of the antifungal agents, nikkomycins[19−21](Figure S1 of the Supporting Information). These studies also demonstrate that active site mutations can lead to large enhancements in both the breadth of substrate specificity and catalytic efficiency and should therefore be targeted in protein engineering experiments.

EXPERIMENTAL PROCEDURES

Construction of the Periplasmic Expression Plasmid. The pBAD/giii-C (Invitrogen) and pUC-ECEDA[22] plasmids were digested with NcoI and XhoI (NEB) in NEB Buffer 4 and bovine serum albumin. The linearized pBAD vector and the *Escherichia coli eda* gene were purified using a 1% agarose gel. The two DNA fragments were combined at equimolar concentrations and ligated using T4 DNA ligase (NEB) to prepare pBAD-giii-ECA. The resulting DNA was transformed into calcium competent SmartCells (Genelantis), and single colonies were picked. After propagation of each colony and isolation of the plasmid DNA, DNA sequencing data were used to confirm that the construct contained the full-length *eda* gene.

Saturation Mutagenesis Libraries. Libraries containing all possible mutations at positions T161, G162, G163, and S184 were made using whole plasmid amplification of the pBAD-giii-ECA construct and the following primers (Integrated DNA Technologies) and their reverse complements: S184X, 5′-GCTGTGCATCGGTGGTNNKTGGCTGGTTCCGGCA-GATGC-3′; T161X, 5′-CCAGGTCCGTTTCTGCCCGNN-KGGTGGTATTTCTCCGGCTAAC-3′; G162X, 5′-GGTC-CGTTTCTGCCCGACGNNKGGTATTTCTCCGGC-TAACTACC-3′; G163X, 5′-GGTCCGTTTCTGCC-CGACGGGTNNKATTTCTCCGGCTAACTACC-3′. The sequence of the position of interest was randomized by allowing the first two nucleotides in the codon to vary (N = A, T, G, or C), and the third position was restricted to G or T (K = G or T).[23] Whole plasmid polymerase chain reaction (PCR) amplification for each library catalyzed by PFU Turbo (Stratagene) was conducted using the primer pair for a single randomized codon under the following thermocycling conditions: one cycle at 95 °C for 30 s; 18 cycles at 95 °C for 30 s, 58 °C for 1 min, and 68 °C for 11 min; and one cycle at 68 °C for 5 min. Following PCR amplification, the template DNA was exhaustively digested overnight with DpnI and the resulting DNA was purified using the Wizard SV Gel and PCR Purification System (Promega). The DNA was transformed into SmartCells and plated on LB/ampicillin plates, yielding hundreds of colonies. All of the colonies were scraped off and

dx.doi.org/10.1021/bi201899b | *Biochemistry* 2012, 51, 1658−1668

pooled together, and the plasmid DNA was purified. Each pool represents libraries of T161, G162, G163, or S184 mutants. DNA sequencing chromatograms of these libraries in aggregate indicated that the targeted sites contained a random assortment of nucleotides according to an NNK distribution. As a second test, the plasmid DNA from three individual colonies per library was isolated and sequenced. All 12 plasmids contained the full-length *eda* gene with different mutations at the targeted sites.

Selection Conditions. The PB25 strain is derived from *E. coli* K12 JM101 and has disruptions in the pyruvate kinase genes, *pykA* and *pykF*; genotype [*supE thi*Δ(*lac-proAB*) *pykA::kan*^{r} *pykF::cat*^{r}].[24] PB25 cells transformed with pBAD-giii-ECA plasmids were plated on selective M9 minimal medium that contained 0.2% ribose, 1 μg/mL thiamine, 40 μg/mL proline, and 50 μg/mL carbenecillin. The plates were augmented with additional nutrients that facilitate growth but do not negate the pyruvate auxotroph phenotype of PB25 cells, including 1 μM $FeCl_3$; 50 μM $ZnSO_4$; 0.1 μM $CaCl_2$; adenosine, guanosine, thymidine, cytosine, and uracil (40 μg/mL each); and D-biotin, cyanocobalamin, folic acid, niacinamide, D-pantothenate, pyridoxal hydrochloride, and riboflavin (1 μg/mL each). The library size was estimated by counting the number of recovered colonies on LB/carbenecillin plates. The plates were also supplemented with 0.1% L-arabinose (to induce expression of the aldolase gene) and 2.5 mM KHO or *S*-KHPB as a source for pyruvate. All colonies plated on selection medium were grown at 34 °C.

As controls, plasmids containing the wild-type aldolase gene were transformed into PB25 cells and plated on selective medium alongside the libraries. No significant background growth was seen on these plates until *S*-KHPB and KHO had been incubated for 72 and 120 h, respectively. All colonies that grew in the first 72 or 120 h on selection plates were picked, restreaked on selective medium, and then grown in 5 mL LB/carbenecillin liquid cultures to recover the plasmid DNA. The DNA was isolated using the Wizard SV Gel and PCR Purification System. The plasmids were retransformed and plated on selective medium to verify that the beneficial activity was associated with the plasmid. The entire *eda* gene was sequenced at the University of Michigan DNA sequencing core.

Construction of Mutants. For ease of expression and purification, the T161S, S184L, and S184F mutants were made in the pET-ECEDA plasmid. The QuikChange (Stratagene) method with the following primers and their reverse complements was used to construct the vectors: T161S, 5′-CCAGGTCCGTTTCTGCCCGTCGGGTGGTATTTCTC-CGGCTAAC-3′; S184F, 5′-GCTGTGCATCGGTGG-TTTCTGGCTGGTTCCGGCAG-3′; S184L, 5′-GCTGTG-CATCGGTGGTCTCTGGCTGGTTCCGGCAG-3′. The pET-ECEDA plasmid[25] encodes the *E. coli eda* gene behind a T7 polymerase promoter and contains an N-terminal hexa-His tag. After whole plasmid PCR amplification with PFU Turbo (Stratagene) and exhaustive digestion with DpnI (NEB), the products were transformed into SmartCells. Following overnight growth on Luria-Bertani medium agar plates containing 100 μg/mL kanamycin, single colonies were cultured and the plasmid DNA was purified and sequenced. The T161S/S184L and T161S/S184F double mutants were constructed from the S184L and S184F plasmids with the primers for the T161S mutation using the whole plasmid PCR amplification method. The sequences of the double mutant plasmids were verified by DNA sequencing.

Protein Expression and Purification. The expression and purification of all KDPG aldolase mutants were conducted according to the protocol previously described[26] using metal affinity chromatography. Briefly, the pET-derived plasmids encoding each mutant *eda* gene were transformed into BL21(DE3) cells, grown on LB/kanamycin (100 μg/mL) plates, and then cultured in Terrific Broth[27] containing 100 μg/mL kanamycin at 37 °C. At an OD_{600} of 0.6−1.0, 1 mM isopropyl β-D-1-thiogalactopyranoside (IPTG) was added and the cultures were incubated for an additional 4−8 h. The cells were pelleted, resuspended in HEPES (25 mM, pH 7.5), and lysed using a Sonic Dismembrator 550 (Fisher Scientific). The crude cell extracts were clarified by centrifugation, and the supernatant was loaded onto a Ni^{2+}-charged Chelating Sepharose Fast Flow (GE Healthcare) column for fractionation using a stepwise gradient of 100 mM HEPES (pH 7.5) and 100 mM NaCl containing 5 mM imidazole (1.5 column volumes), 155 mM imidazole (2 column volumes), and 500 mM imidazole (2 column volumes). Fractions containing the His-tagged KDPG aldolase eluted during the 500 mM imidazole wash. These fractions were combined and concentrated using Amicon Ultra (Millipore) spin concentrators and extensively washed with 100 mM HEPES (pH 7.5) and 100 mM NaCl to remove the imidazole. Enzymes stored at 4 °C in 100 mM HEPES (pH 7.5), 100 mM NaCl, and 10% glycerol, at concentrations of 1−5 mM, are stable for up to 1 year.

The protein concentrations were determined by absorbance at OD_{280} where the extinction coefficient (ε_{280}) was calculated to be 15510 M^{-1} cm^{-1} for both wild-type and mutant KDPG aldolases. The protein concentrations and purity were confirmed by 12% polyacrylamide gel electrophoresis followed by Coomassie staining and comparison of band intensity to a known standard.

Kinetic Assay for Retro-Aldol Cleavage. The mutants were assayed for retro-aldol cleavage of KDPG and related analogues (KDPGal, KHO, *S*-KHPB, and *R*-KHPB) using a lactate dehydrogenase (LDH)-coupled assay in which the initial velocity for the production of pyruvate was measured by the decrease in NADH absorbance at 340 nm (ε = 6220 M^{-1} cm^{-1}). All assays were conducted using a CARY 100 Bio UV−vis spectrometer fitted with a Peltier temperature controller in quartz microcuvettes (70 μL) at 25 °C. The reaction mixtures contained the following final concentrations: 100 mM HEPES (pH 7.5), 250 μM NADH, 0.023 unit/μL LDH (Sigma), 50 μM to 50 mM KDPG (or analogues), depending on the K_M value, and 50 nM to 10 μM enzyme, depending on the k_{cat} value. Data were collected in three replicates. The Michaelis−Menten equation was fit to the data using the curve fitting program GraphPad PRISM 4, and standard errors were determined.

Specificity Assay with Various Electrophiles. Stopped point assays were conducted to measure the efficiency of aldol synthesis by reaction of various aldehydes with pyruvate catalyzed by the T161S/S184L and wild-type KDPG aldolases. Each reaction mixture contained 200 mM HEPES (pH 7.5), 4 mM pyruvate, and 50 mM aldehyde (D-GAP, D,L-glyceraldehydes, 2-, 3-, or 4-pyridine carboxaldehyde, valeraldehyde, benzaldehyde, 2-furaldehyde, or D- or L-erythrose). The stock solutions for benzaldehyde and 2-furaldehyde contained 20% DMSO to improve solubility in water, and 10% DMSO was maintained in the reaction vessel for these two substrates. An aliquot was removed prior to adding the enzyme to serve as a zero point for the assay. The reaction was initiated

by addition of enzyme (1 μM enzyme for D-GAP; 10 μM enzyme for glyceraldehyde and 2-pyridine carboxaldehyde, and 50 μM enzyme for the rest of the aldehydes), and the linear increase in the amount of product was monitored for a maximum of 3 h. At 30 min intervals, an aliquot of the reaction mixture was diluted 20-fold into 100 mM HEPES (pH 7.5) and 300 μM NADH. The change in absorbance at 340 nm after addition of 0.8 unit of LDH was measured to assay the remaining pyruvate concentration. The time-dependent decrease in the amount of pyruvate was used to calculate the initial velocity for the reaction of pyruvate with each electrophile. Two independent replicates were conducted, and the initial velocity data were averaged.

Synthesis of Substrates. The syntheses of 2-keto-3-deoxy-6-phosphogluconate (KDPG), 2-keto-4-hydroxy-octonoate (KHO), and (4*S*)-2-keto-4-hydroxy-4-(2′-pyridyl)butyrate (*S*-KHPB) were previously reported.[22,26] 2-Keto-3-deoxy-6-phosphogalactonate (KDPGal) and (4*R*)-2-keto-4-hydroxy-4-(2′-pyridyl)butyrate (*R*-KHPB) with high enantiomeric purity were synthesized enzymatically using KDPGal aldolase as previously described[28] and were gifts from M. J. Walters (Duke University).

Construction of Substrate Binding Models for KDPG Aldolases. Substrates were modeled into the published structures of *E. coli* KDPG aldolase [Protein Data Bank (PDB) entry 1EUA[29]] using Accelrys Viewer Pro version 4.2. The coordinates for the backbones of KDPGal-Schiff base (taken from the structure of KDPGal aldolase, PDB entry 2V82[28]) were superimposed on the KDPG aldolase structure. The stereochemistry of the C4 hydroxyl was inverted, and the C−C torsions were adjusted to avoid van der Waals contacts with the protein side chains. The torsion angles for the modeled KDPG substrate are −178° (C1−C2), −93° (C2−C3), 171° (C3−C4), 109° (C4−C5), 102° (C5−C6), and 93° (C6−O6). The position of water W1 is inferred from the position of the carbinolamine oxygen, as described by Fullerton et al.[30] Water W1 was moved (up to 2 Å) to a position that approximates ideal geometries for proton transfer steps. No protein side chain positions were modified in this model.

The model of 2-pyridine carboxaldehyde bound to KDPG aldolase was generated using the drawing tools in Viewer Pro version 4.2. The molecule was superimposed on the KDPG aldolase structure and adjusted to avoid van der Waals contacts and to maximize the orientation and geometry required for the aldol addition reaction. The torsion angle between Cα and C1 is 50°. The pyruvyl-enamine was modeled on the basis of the structure of the pyruvyl-Schiff base[30] where the K133 Cδ−Cε and Cε−Nζ dihedral angles were modified by 10° and −26°, respectively, to avoid van der Waals clashes between the pyruvyl C3 atom and the aldehydic Cα atom. Consequently, the pyruvyl C3 atom is ∼1.2 Å farther from the aldehyde binding pocket than the equivalent carbon of the pyruvyl-carbinolamine observed in the 1EUA crystal structure. Moving these atoms does not create any steric clashes or significantly alter the position of the pyruvyl C1 carboxylate. The double-mutant model was made by deleting the methyl side chain of T161 and replacing S184 with leucine using the drawing tools in Viewer Pro version 4.2 and adjusting the torsions to minimize steric contacts.

RESULTS

Identification of KDPG Aldolase Mutants with Altered Substrate Selectivity. We previously reported an active site mutation in KDPG aldolase that markedly improves the catalytic efficiency of aldol addition between pyruvate and 2-pyridine carboxaldehyde. In this mutant, serine 184, located in the phosphate binding site of KDPG aldolase, is substituted with leucine, which enhances the reactivity of this enzyme with hydrophobic electrophiles, such as 2-pyridine carboxaldehyde, by up to 40-fold.[26] These mutagenesis data combined with structural studies identified the aldehyde binding pocket, allowing the use of structure-based approaches in redesigning the substrate specificity of KDPG aldolase.[26,30] On the basis of these studies, we mutagenized key amino acids that line the aldehyde binding loop to identify alterations that enhance reactivity with hydrophobic substrates.

Examination of every possible variant at every position for even a small enzyme like KDPG aldolase (213 amino acids) would require an astronomically large library (∼20^{200} molecules). Limiting the variability to amino acids that are within 5 Å of the active site still results in an intractable library size of ∼20^{30}. Reasoning that alterations in residues that directly contact the substrate are more likely to alter substrate selectivity than distal amino acids, we limited the complexity of our libraries by varying only active site residues. On the basis of structural insights into the aldehydic substrate binding site,[26,30] we targeted four positions for mutagenesis: G162, G163, and S184, residues located on two loops that form the phosphate binding site, and T161, which bridges the pyruvate and aldehydic binding pockets and contributes to the stereospecificity of the enzyme[28] (Figure 2). The in vivo

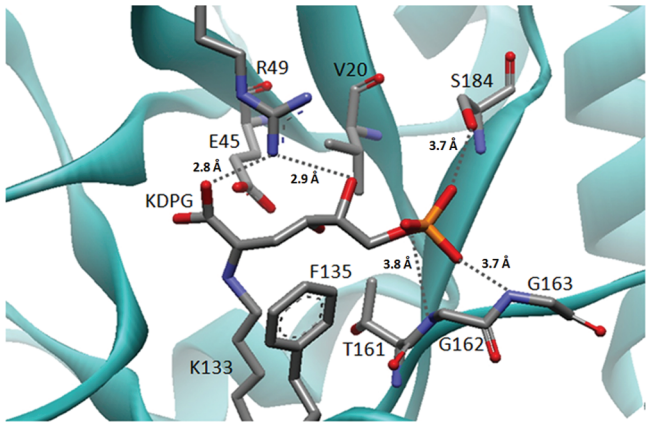

Figure 2. Model of KDPG bound as a Schiff base to *E. coli* KDPG aldolase. The model was built using PDB entry 1EUA[29] as described in Experimental Procedures, and the substrate conformation resembles the structure of KDPGal bound to *E. coli* KDPGal aldolase.[28] Proposed hydrogen bonds are denoted with gray dashed lines and distances. The catalytic waters have been omitted for the sake of clarity.

activity of the mutants encoded in these libraries was examined using a previously developed *E. coli* selection system based on a pyruvate auxotrophic strain (PB25).[22] This strain is unable to grow on minimal ribose plates without supplemental pyruvate.[24] Augmentation of selection plates with a compound that is cleaved by a mutant KDPG aldolase to generate pyruvate facilitates cell survival. Previous data suggested that this selection method mainly identifies enhancements in substrate binding caused, presumably, by the low in vivo concentration of the substrates.[15] To circumvent this issue, KDPG aldolase was fused to the signal sequence from the filamentous phage fd pIII gene that localizes the protein to the periplasm[31] where the

dx.doi.org/10.1021/bi201899b | *Biochemistry* 2012, 51, 1658−1668

substrate concentration reflects the concentration in the medium. Using this method, *E. coli* KDPG aldolase variants were selected for improved catalysis of two hydrophobic analogues of KDPG: (1) 2-keto-4-hydroxy-octonoate (KHO), a hydrophobic analogue that lacks the C5 hydroxyl and C6 phosphate of KDPG, and (2) (4*S*)-2-keto-4-hydroxy-4-(2′-pyridyl)butyrate (*S*-KHPB), an analogue containing a pyridyl group that is an important precursor for nikkomycin synthesis (Figure 3).

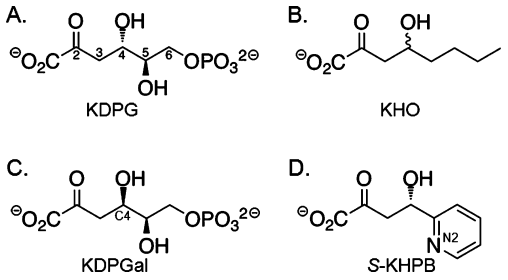

Figure 3. Substrates for KDPG aldolase used in this study. (A) 2-Keto-3-deoxy-6-phosphogluconate (KDPG) is the natural *gluco* sugar substrate. (B) 2-Keto-4-hydroxy-octonoate (KHO) is a hydrophobic analogue that lacks the C5 hydroxyl and C6 phosphate. (C) 2-Keto-3-deoxy-6-phosphogalactonate (KDPGal) differs from KDPG by only the stereochemistry at C4. (D) (4*S*)-2-Keto-4-hydroxy-4-(2′-pyridyl)-butyrate (*S*-KHPB) is a reactive analogue.

To identify mutations that enhance reactivity with hydrophobic substrates, we prepared four libraries with the sequence of the codons at positions 161−163 and 184 individually randomized. By employing NNK degeneracy (N, all nucleotides; K, only guanosine and thymidine) in the primers, these libraries contain a total library size of 32 variants that encode all 20 amino acids and a stop codon. For such small libraries, screening 100 variants provides a 95% confidence level that every possible amino acid substitution has been examined.[32] The mutant plasmid libraries were transformed into PB25 cells, plated on KHO or *S*-KHPB selection medium, and incubated for 72 h. More than 100 clones were plated from each library, providing a high degree of confidence that all possible substitutions were examined. A small number of colonies (zero to three) were isolated from each selection plate (Table S2 of the Supporting Information), and the KDPG gene encoded on each plasmid was sequenced. Three single-amino acid mutants were obtained from plasmids selected by growth on KHO plates: T161S, G162V, and S184F. Only one mutation conferred growth on the *S*-KHPB selection plates, namely T161S. Unexpectedly, in this screen, we did not identify the S184L mutation that we had previously demonstrated enhanced reactivity of this enzyme with 2-pyridine carboxaldehyde.[26] This result suggests that another variable, such as the stability or expression level of the S184L mutant compared to that of the S184F mutant, limited the ability to confer growth under the selection conditions.

The biochemical properties of the selected mutant KDPG aldolases were analyzed. All three mutants are expressed at a high level in *E. coli*. The T161S and S184F mutants were both easily purified, but the G162V KDPG aldolase mutant precipitated during purification and was not analyzed further. To measure changes in substrate selectivity for the T161S and S184F mutants, we determined the kinetic parameters for catalysis of retro-aldol cleavage of KDPG, KHO, and *S*-KHPB (Table 1). The specificity constant (k_{cat}/K_M) is the most important parameter for consideration of substrate selectivity and catalytic efficiency, while the turnover number may be most informative for identifying efficient biocatalysts. The steady state kinetic parameters for retro-aldol cleavage of KHO and *S*-KHPB catalyzed by wild-type KDPG aldolase (Table 1) indicate that the catalytic efficiency (k_{cat}/K_M) is decreased by 10^4−10^5-fold relative to KDPG because of both decreases in the value of k_{cat} and increases in K_M. Although K_M frequently includes multiple terms and may not simply reflect binding affinity, the high value of this parameter coupled with the low turnover number suggests that wild-type KDPG aldolase binds these alternate substrates with low affinity.

The T161S mutation improves the value of k_{cat}/K_M^{KHO} for catalyzing cleavage of KHO by 8-fold, largely because of a 10-fold decrease in the value of K_M^{KHO} (Table 1). The T161S mutation causes an even greater enhancement of catalysis of retro-aldol cleavage of *S*-KHPB; the value of $k_{cat}/K_M^{S\text{-}KHPB}$ increases by 12-fold compared to the value for wild-type KDPG aldolase. Remarkably, this enhancement is caused by a 16-fold increase in the value of the turnover number. However, the T161S mutation does not increase the reactivity of KDPG aldolase with all substrates. This mutant has little effect on the catalytic efficiency with the natural substrate, KDPG, leading to comparable decreases in the values of k_{cat}^{KDPG} and K_M^{KDPG} (3- and 2-fold, respectively). Despite the large increases

Table 1. Kinetic Parameters for Cleavage of KDPG, KHO, and *S*-KHPB Catalyzed by *E. coli* KDPG Aldolase Mutants[a]

	KDPG			KHO[b]			*S*-KHPB		
	k_{cat} (s^{-1})	K_M (mM)	k_{cat}/K_M (M^{-1} s^{-1})	k_{cat} (s^{-1})	K_M (mM)	k_{cat}/K_M (M^{-1} s^{-1})	k_{cat} (s^{-1})	K_M (mM)	k_{cat}/K_M (M^{-1} s^{-1})
wild type[c]	83 (2)	0.10 (0.01)	830000 (20000)	2.0[d] (0.6)	146[d] (50)	14[d] (1)	11 (1)	32 (2)	330 (9)
T161S	27 (1)	0.05 (0.01)	550000 (65000)	1.7 (0.2)	15 (4)	113 (20)	175 (40)	43 (12)	4100 (800)
S184F	40 (2)	1.7 (0.2)	24000 (2000)	1.5 (0.1)	25 (4)	60 (4)	19 (1)	5.7 (0.8)	3300 (60)
S184L[c]	74 (7)	0.35 (0.10)	210000 (10000)	2.9 (0.2)	26 (4)	110 (10)	40 (1)	3.0 (0.2)	13000 (600)
T161S/S184F	31 (2)	0.69 (0.06)	45000 (2500)	[e]	[e]	[e]	212 (12)	3.5 (0.5)	61000 (5000)
T161S/S184L	41 (2)	0.24 (0.04)	170000 (27000)	3.1 (0.2)	4.3 (0.7)	720 (90)	240 (11)	1.6 (0.2)	150000 (16000)

[a]The initial velocity for pyruvate formation was measured using a lactate dehydrogenase-coupled assay as described in Experimental Procedures. Steady state kinetic parameters were determined by a fit of the Michaelis−Menten equation to the initial velocity as a function of substrate concentration. These assays were conducted at 25 °C. Errors are shown in parentheses. [b]KHO is synthesized in racemic form, and the indicated concentration includes both C4 stereoisomers. Because KDPG aldolase preferentially catalyzes the cleavage of (*S*)-KHO, the measured K_M is likely to be higher than the actual value for (*S*)-KHO. Consequently, the k_{cat}/K_M is an underestimate of the actual value. [c]These data were previously published.[26] [d]The initial velocity has a nearly linear dependence on the concentration of KHO up to the maximal measurable concentration of 50 mM. [e]Data were not collected.

dx.doi.org/10.1021/bi201899b | *Biochemistry* 2012, 51, 1658−1668

in the catalytic efficiency of KHO and *S*-KHPB cleavage, the T161S mutant retains selectivity for KDPG, with a cleavage efficiency (k_{cat}/K_M^{KDPG}) that is >100-fold larger than that of either of the other substrates.

The S184F mutation also significantly alters the substrate specificity of this aldolase, increasing the values of k_{cat}/K_M^{KHO} and $k_{cat}/K_M^{S\text{-}KHPB}$ by 4- and 10-fold, respectively, mainly through lowering the value of K_M, yet these enhancements in catalytic efficiency are 2−4-fold smaller than those observed for the S184L mutant previously measured[26] (Table 1). However, while the S184L mutation has a small effect (4-fold decrease) on the reactivity with KDPG, the S184F variant decreases the value of k_{cat}/K_M^{KDPG} by ∼35-fold, mainly by increasing the value of K_M^{KDPG}. Therefore, the S184F substitution significantly increases the selectivity for cleavage of KHO and *S*-KHPB relative to KDPG compared to that of the S184L variant. These data are consistent with the proposal that the side chain at position 184 forms a portion of the aldehyde binding pocket[26] (Figure 2). Substitution of Ser184 with Phe or Leu presumably increases the hydrophobicity of the binding pocket, thereby improving the catalytic efficiency with hydrophobic aldehydes. However, the larger size of the Phe side chain compared to that of Leu or Ser interferes with the apparent binding affinity of KDPG.

Alterations in Substrate Selectivity Are Additive in Double Mutants. Because the T161S mutation primarily enhances the k_{cat} parameter while the S184L and -F mutations lower the K_M parameter, the effects of these mutations could be additive; i.e., the first mutation makes beneficial contacts with the substrate, while the second improves the cleavage efficiency of the bound substrate. To examine whether these mutations have an additive effect on catalysis, we prepared and purified two double mutants, T161S/S184L and T161S/S184F KDPG aldolase. Both proteins were readily expressed and stable.

Combining mutations at positions 161 and 184 enhances the specificity of the aldolase for cleavage of KHO and *S*-KHPB relative to KDPG beyond that of either mutation alone. The T161S/S184L variant shows the most pronounced alterations in substrate selectivity. The value of k_{cat}/K_M^{KHO} for cleavage of KHO is improved by >50-fold compared to that of the wild-type KDPG aldolase. Furthermore, these substitutions enhance the catalytic efficiency of *S*-KHPB cleavage by >450-fold, resulting in a value of k_{cat}/K_M^{KHPB} that approaches (18%) the activity of the wild-type enzyme with KDPG. Because most biocatalytic processes are run under conditions where substrate is abundant, improving the turnover number is arguably the most important aspect of protein engineering, at least with respect to synthetic applications. Remarkably, the T161S/S184L mutant enhances the value of $k_{cat}^{S\text{-}KHPB}$ for cleavage of *S*-KHPB by 22-fold, such that the turnover number (240 s^{-1}) is nearly 3 times greater than that of wild-type KDPG aldolase with its natural substrate (83 s^{-1}). The T161S/S184L mutant also retains significant activity with KDPG; the value of k_{cat}/K_M^{KDPG} decreases by less than 5-fold. Therefore, the T161S and S184L mutations significantly broaden the substrate selectivity of this aldolase, with comparable activities for KDPG and *S*-KHPB cleavage and enhanced activity with KHO (Figure 4A).

The T161S/S184F double mutant shows a trend similar to that observed for T161S/S184L aldolase; however, the enhancement of *S*-KHPB cleavage efficiency is smaller (∼180-fold), while the reduction in KDPG cleavage efficiency is more substantial (18-fold). As a result, the T161S/S184F mutant has a larger change in selectivity, altering the substrate selectivity ratio[a] between KDPG and *S*-KHPB by 3400-fold (Table 2). These data are similar to the effects observed in the S184F single mutant and are consistent with the phenylalanine substitution at position 184 partially occluding the KDPG binding site.

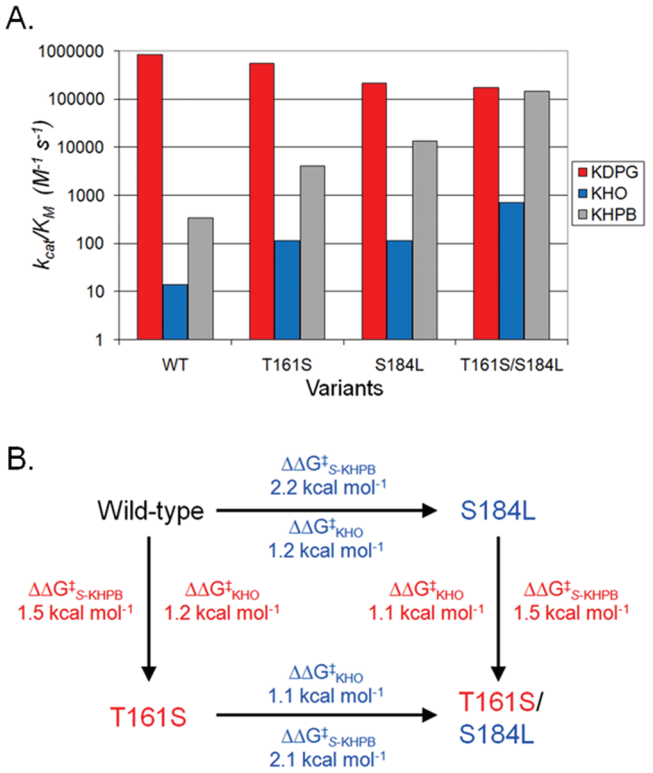

Figure 4. (A) Comparison of k_{cat}/K_M values for *E. coli* KDPG aldolase wild-type and mutant enzymes with KDPG, KHO, and *S*-KHPB. The catalytic efficiencies are shown for KDPG cleavage (red), KHO cleavage (blue), and *S*-KHPB (gray). (B) Additive effect of individual mutations in the T161S/S184L mutant on the catalytic efficiency of KHO and *S*-KHPB. $\Delta\Delta G^{\ddagger} = -2.303RT \log[(k_{cat}/K_M^{variant\ 1})/(k_{cat}/K_M^{variant\ 2})]$, where T = 298.15 K and R = 1.987 cal K^{-1} mol^{-1}.

To further probe the substrate specificity of the T161S/S184L mutant, we measured the catalytic rate constant in the synthetic direction for the reaction of pyruvate and various electrophilic substrates at saturating concentrations of pyruvate (4 mM) and high concentrations of the aldehyde, mimicking plausible conditions for a synthetic application (Table 3). The most striking result is the switch in the identity of the highest-activity aldehydic substrate from D-glyceraldehyde 3-phosphate for wild-type KDPG aldolase to 2-pyridine carboxaldehyde (2-PCA) for the T161S/S184L mutant, equivalent to a 24-fold change in selectivity[b] for reaction with these two substrates.

Table 2. Changes in Substrate Selectivity of *E. coli* KDPG Aldolase Mutants[a]

	substrate selectivity compared to KDPG cleavage	
	KHO	*S*-KHPB
wild-type	1	1
T161S/S184L	250	2200
T161S/S184F	–	3400

[a] Selectivity ratio = $[(k_{cat}/K_M^{KDPG})/(k_{cat}/K_M^{X})]^{wild\text{-}type}/[(k_{cat}/K_M^{KDPG})/(k_{cat}/K_M^{X})]^{mutant}$.

dx.doi.org/10.1021/bi201899b | *Biochemistry* 2012, 51, 1658−1668

Table 3. Catalysis of the Aldol Reaction between Pyruvate and Various Aldehydes by *E. coli* KDPG Aldolase and the T161S/S184L Mutant[a]

substrate	wild-type enzyme	T161S/S184L enzyme	change in selectivity[b]
D-glyceraldehyde 3-phosphate	100%	15%	–
DL-glyceraldehyde	4%	1%	1.7
D-erythrose	0.3%	0.03%	0.67
L-erythrose	0.06%	0.03%	3.3
2-pyridine carboxaldehyde	25%	89%	24
3-pyridine carboxaldehyde	0.5%	1%	13
4-pyridine carboxaldehyde	3%	2.5%	5.6
valeraldehyde	0.005%	0.008%	11
2-furaldehyde	0.005%	0.003%	4.0
benzaldehyde	0%	0%	–

[a]This assay was conducted with 4 mM pyruvate and 50 mM aldehyde substrate. All of the data in this table were normalized to the activity of wild-type KDPG aldolase with its natural electrophilic substrate, D-glyceraldehyde 3-phosphate. [b]$(\text{activity}^{\text{aldehyde}}/\text{activity}^{\text{D-GAP}})^{\text{mutant}}/(\text{activity}^{\text{aldehyde}}/\text{activity}^{\text{D-GAP}})^{\text{wild-type}}$.

In general, under these assay conditions, reactivity with sugar electrophiles decreases (2−10-fold) in the mutant, while reactivity with more hydrophobic aldehydes is unchanged or increases, leading to a net increase in selectivity for hydrophobic aldehydes of 4−24-fold (Table 3). However, the selectivity for 2-PCA is the highest, suggesting that the selection identified a mutant that both broadens the specificity of the aldolase and forms a specific interaction with 2-PCA to enhance the reactivity with this substrate.

Aldolase Mutants Retain Stereoselectivity. One important aspect of developing aldol catalysts for biocatalytic uses is to maintain the stereospecificity of the native reaction. To examine this property, we compared the efficiency of mutant aldolases for aldol cleavage of substrates with epimeric C4 stereocenters: KDPG versus KDPGal and *S*-KHPB versus *R*-KHPB (Table 4). The T161S mutation increases the reactivity for cleaving KDPGal, reducing the observed stereoselectivity ratio[c] from the wild-type value of 14000 to 710. In contrast, the S184L substitution causes a larger decrease in the reactivity with KDPGal than with KDPG, thus increasing the stereoselectivity ratio by >5-fold compared to that of wild-type KDPG aldolase. A priori, it was not clear how each of these effects would contribute to the stereoselectivity of the double mutants. However, the T161S/S184L double mutation also decreases the rate of KDPGal cleavage to a greater extent than the rate of KDPG cleavage (Table 4), leading to a stereoselectivity ratio that is almost 2-fold higher than that of the wild-type enzyme. Similar behavior is observed for the T161S/S184F mutant (data not shown). These data further suggest that the effects of the two mutations on substrate selectivity are roughly additive. Additionally, the two double mutants enhance the stereoselectivity ratio[d] for cleavage of *R*-KHPB up to 150-fold relative to the wild-type aldolase (Table 4). Although the mutations slightly enhance (up to 3-fold) the reactivity with *R*-KHPB, the substantially larger increases in the rate of catalysis of cleavage of *S*-KHPB lead to increased enantioselectivity. The high activity and stereoselectivity of these mutants make them particularly useful for the stereospecific synthesis of pharmaceuticals and other high-value specialty and commodity chemicals.

DISCUSSION

On the basis of structure-guided mutagenesis, we previously prepared an active site mutant in KDPG aldolase (S184L) that markedly improves the catalytic efficiency of *S*-KHPB retroaldol cleavage and enhances the reactivity with nonphosphorylated electrophiles.[26] Alteration of the serine residue located in the phosphate binding site of KDPG aldolase presumably enhances contacts between the hydrophobic tail of the substrate and the aldehydic substrate binding pocket to increase catalytic efficiency. Here we use targeted mutagenesis coupled with selection methods to identify two additional mutations that improve the catalytic efficiency of this enzyme for cleavage of *S*-KHPB. The S184F mutation most likely enhances the catalytic efficiency for hydrophobic electrophiles in a manner similar to that of S184L, by improving contacts with the substrate. Because the T161S mutation mainly increases the turnover number (k_{cat}) rather than the apparent binding affinity (K_M), this mutation has a different mode of action.

The side chains of S184 and T161 are 7 Å apart, and mutations at these positions largely affect different steady state kinetic parameters. Therefore, these mutations might work independently and provide complementary benefits in substrate

Table 4. Kinetic Parameters for Cleavage of KDPGal and *R*-KHPB Catalyzed by *E. coli* KDPG Aldolase Mutants[a] and Enantiomeric Selectivity Ratios

	k_{cat} (s^{-1})	K_M (mM)	k_{cat}/K_M (M^{-1} s^{-1})	stereoselectivity ratio[b]
		KDPGal		
wild-type[c]	0.0063 ± 0.0001	0.10 ± 0.01	61 ± 3	14000
T161S	0.23 ± 0.02	0.3 ± 0.05	770 ± 90	710
S184L[c]	0.0026 ± 0.0001	0.95 ± 0.17	2.7 ± 0.4	78000
T161S/S184L	0.0060 ± 0.0008	1.0 ± 0.1	6.5 ± 0.7	26000
		R-KHPB[d]		
wild-type	–	>50	0.01 ± 0.003	33000
T161S/S184F	–	>50	0.017 ± 0.008	3600000
T161S/S184L	–	>50	0.03 ± 0.004	5000000

[a]The kinetic parameters were measured as described in the footnotes of Table 1. [b]The stereoselectivity ratio is defined as $(k_{cat}/K_M^{KDPG})/(k_{cat}/K_M^{KDPGal})$ or $(k_{cat}/K_M^{S\text{-KHPB}})/(k_{cat}/K_M^{R\text{-KHPB}})$. Values for k_{cat}/K_M^{KDPG} and $k_{cat}/K_M^{S\text{-KHPB}}$ are listed in Table 1. [c]These data were previously published.[26] [d]The initial velocity is linearly dependent on the concentration of *R*-KHPB up to 50 mM, allowing measurement of only the value of k_{cat}/K_M.

dx.doi.org/10.1021/bi201899b | *Biochemistry* 2012, 51, 1658−1668

binding and catalysis. In accord with this hypothesis, the contributions from each mutation are largely additive in the double mutants, as illustrated in Figure 4B for T161S/S184L. The T161S mutation decreases the activation energy for *S*-KHPB catalysis ($\Delta\Delta G^{\ddagger}_{S\text{-KHPB}}$) by 1.5 kcal/mol.[e] The analogous mutation in the S184L background (T161S/S184L mutant) yields a $\Delta\Delta G^{\ddagger}_{S\text{-KHPB}}$ of 1.4 kcal/mol compared to that of the reaction catalyzed by the S184L variant. Likewise, the S184L mutation in the wild-type background decreases the activation energy by 2.2 kcal/mol, while the same mutation in the T161S mutant results in a 2.1 kcal/mol change in $\Delta\Delta G^{\ddagger}_{S\text{-KHPB}}$. Catalysis of KHO cleavage reflects a similar trend for $\Delta\Delta G^{\ddagger}_{KHO}$ (Figure 4B). On the other hand, the effect on stereoselectivity does not show a consistent quantitative pattern. Although the T161S mutation reduces the stereoselectivity of the enzyme while the S184L mutation increases stereoselectivity, the magnitude of the effect is dependent on the context. This result suggests stereoselectivity in this enzyme is determined by complex protein−substrate recognition, rather than by interactions at a single key location. In contrast, the stereoselectivity of BphI aldolase (a class II metal-dependent enzyme) is controlled mainly by a single residue.[11]

Origin of Stereoselectivity in KDPG Aldolase. Because KDPG aldolase and a structural homologue, KDPGal aldolase, catalyze aldol addition of substrates differing only in their facial selectivity of addition, a comparison of these enzymes might provide insight into the structural basis of stereochemical control. Previous studies of KDPG[29] and KDPGal aldolases[28] identified numerous subtle differences in the active sites of these two proteins and demonstrated that mutation of the residue at position 161 (equivalent to V154 in KDPGal aldolase) alters the overall stereoselectivity of the two enzymes.[28] In particular, the T161A mutant in KDPG aldolase relaxes the stereoselectivity of the mutant enzyme more than 3000-fold by both enhancing KDPGal cleavage and decreasing KDPG cleavage rates. Furthermore, mutation of T161 to valine essentially abolished catalytic activity for both epimeric sugars. In contrast, the T161S mutant identified in this work using selection methods retains significant enantioselectivity (Table 4) because the efficiency of cleaving KDPGal increases modestly (13-fold) without adversely affecting the reaction with KDPG. Taken together, these data suggest that a hydroxyl group at position 161 plays an important role in determining stereoselectivity.

To clarify the role of T161 in stereoselectivity, we constructed models of enzyme−substrate complexes. On the basis of the crystal structure of KDPGal bound to *E. coli* KDPGal aldolase (PDB entry 2V82[28]), we modeled the *gluco* sugar, KDPG, bound as a Schiff base in the active site of *E. coli* KDPG aldolase (PDB entry 1EUA[29]) (Figure 2). We further postulated that the two substrates bind in similar orientations, and no major conformational shifts occur during the catalytic cycle so that the positions of the side chains are unchanged. (This is a reasonable assumption because all crystal structures of KDPG and KDPGal aldolases with or without bound substrates have similar overall folds with only minor differences in the orientation of catalytic residues.[28−30]) In this model, the C4 (epimeric carbon) hydroxyl of KDPG points down into the cavity toward the methyl group of T161 (Figure 5A). This conformation is stabilized by interaction of the C4 hydroxyl (O4) directly with water W1 and indirectly with water W2 via W1. (W2 is unique to KDPG aldolases and is not observed in KDPGal aldolases. In the crystal structure,[29] W2 forms hydrogen bonds with T161 and E45 and is positioned to form a hydrogen bond with W1.) In this model of the *gluco* sugar, W1 is positioned to mediate the transfer of a proton from O4 to E45 (distance of 2.8 Å and proton abstraction angle of 125°) to initiate retro-aldol cleavage (Scheme 1). By contrast, in a model similarly constructed of the *galacto* sugar bound to KDPG aldolase, the C4 hydroxyl points toward R49 where unfavorable van der Waals contacts with R49 and the side chain of V20 are likely (Figure 5A and Figure S2 of the Supporting Information). Furthermore, in this model, W1 is poorly positioned to facilitate proton transfer (distance of 3.8 Å and proton abstraction angle of 76°). These models provide a rationale for the enhanced affinity and reactivity of KDPG

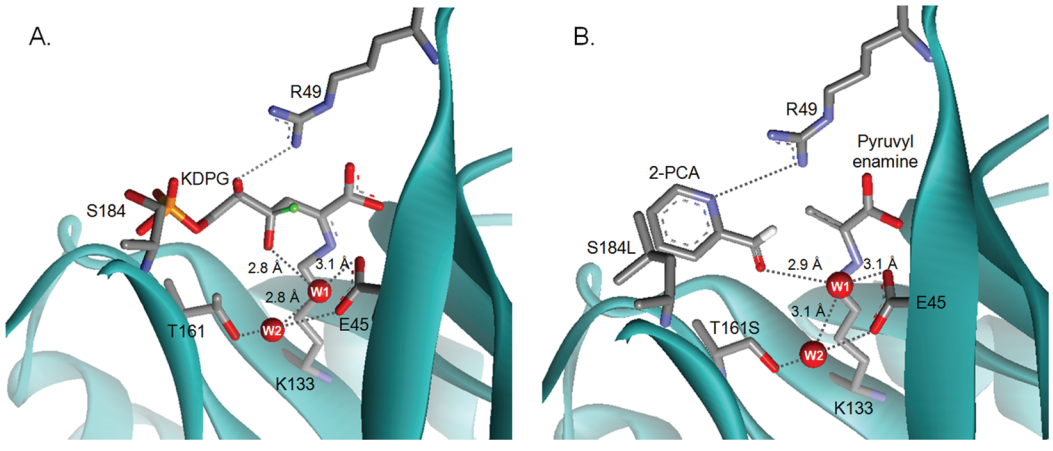

Figure 5. Models of substrates bound to *E. coli* KDPG aldolase. (A) Model of KDPG bound to the active site of KDPG aldolase. A proposed hydrogen bond network of waters that stabilize the complex is shown in gray dashed lines with key distances indicated. Water W1 is proposed to preferentially enhance the affinity of the *gluco* sugar and mediate catalytically important proton transfer steps. Water W2 is proposed to help position W1. The C4 hydroxyl from a model of a *galacto* sugar bound to KDPG aldolase is superimposed as a green ball. This model suggests that the *galacto* epimer is a less efficient substrate for KDPG aldolase because O4 bumps into R49, the angle for deprotonation of O4 by W1 is poor, and the distance between these atoms is long (3.8 Å). (B) Model of 2-PCA bound to the T161S/S184L mutant. The model suggests that hydrophobic contacts are made between the aromatic heterocycle of 2-PCA and leucine at position 184 and that the T161S mutation removes a steric clash with the aldehydic oxygen of 2-PCA. Also, the side chain of R49 is positioned to form a hydrogen bond with N2 of 2-PCA, similar to the hydrogen bond between O4 of KDPG and R49.

dx.doi.org/10.1021/bi201899b | *Biochemistry* 2012, 51, 1658−1668

aldolase with the *gluco* versus *galacto* sugar as well as the effects of mutations at T161. We posit that the T161S mutant preserves the hydrogen bond network among E45, W1, and W2 and therefore maintains a high efficiency for catalyzing KDPG cleavage (Table 1). However, the threonine to serine mutation widens the tunnel to the active site, allowing for increased substrate promiscuity.

A role for catalytic waters has been proposed for many class I aldolases,[30,33−37] while a role for water in controlling stereochemistry has been suggested in the tagatose-1,6-bisphosphate and fructose-1,6-bisphosphate aldolases.[35] Likewise, in KDPGal aldolase, subtle structural differences in the active site position W1 differently than in KDPG aldolase, making occupancy of the upper site by O4 preferred and presumably giving rise to the preference for reaction with substrates containing inverted C4 stereochemistry (see Figure S3 of the Supporting Information for an explanation of the KDPGal stereoselectivity). The careful positioning of water to mediate stereospecific proton transfers may be a common strategy in class I aldolase enzymes.

Improving Activity with 2-Pyridine Carboxaldehyde. Remarkably, the T161S/S184L mutant has a maximal turnover number for retro-aldol cleavage of *S*-KHPB that is 3 times higher than that of the wild-type enzyme with any substrate (Table 1), and 2-PCA is the best electrophilic substrate for the mutant enzyme (Table 3). The enhanced reactivity of 2-PCA with the T161S/S184L KDPG aldolase mutant can be rationalized by modeling the structure of 2-PCA at the active site of pyruvate-bound wild-type and mutant *E. coli* KDPG aldolase,[29] assuming that the protein structure was unchanged [except for minor rotations around the Schiff base lysine (K133) Cδ−Cε and Cε−Nζ dihedral angles]. The model of 2-PCA bound to the wild-type enzyme suggests that steric interactions between the methyl group of T161 and the substrate aldehyde do not allow the formation of optimal reaction distances between the nucleophilic C3 in pyruvate and the electrophilic carbon in 2-PCA (pyruvate C3−2-PCA Cα distance of 4.3 Å). The hydrogen bond between W1 and the carbonyl oxygen of 2-PCA (distance of 3.5 Å) is also too long for efficient catalysis. In the model of PCA bound to the T161S/S184L mutant (Figure 5B), N2 of the pyridyl moiety of 2-PCA forms a hydrogen bond with the side chain of R49 and the aldehydic oxygen is positioned in the hole left by removal of the methyl group of T161. This repositioning of 2-PCA decreases the distance between the reacting carbon atoms (C3−Cα distance of 3.3 Å) and shortens the hydrogen bond with W1 to 2.9 Å, presumably enhancing the catalytic activity. Furthermore, the S184L substitution is positioned to make hydrophobic contacts with the aromatic ring of 2-PCA, as previously suggested by structure−reactivity studies of mutations at this position.[26] This proposed binding configuration provides a reasonable explanation for the enhanced reactivity of the mutant enzymes with *S*-KHPB.

The models of the KDPG aldolase−substrate complexes also suggest that the side chain of R49 forms a hydrogen bond with the C5 hydroxyl of KDPG (Figures 2 and 5A) or N2 of the aromatic ring of 2-PCA. An analogous hydrogen bond between the C5 hydroxyl of KDPGal and R17 has been observed in the crystal structure of KDPGal aldolase complexed with a substrate.[28] The low reactivity of KDPG aldolase with substrates incapable of forming a hydrogen bond with R49, including 3-PCA, 4-PCA, valeraldehyde, and benzaldehyde (Table 3), suggest that this interaction is important for activity. Consistent with this, deletion of the arginine 49 side chain in the R49A mutant of KDPG aldolase decreases the efficiency of retro-aldol cleavage of KDPG enormously (2.3×10^4-fold; $k_{cat}/K_M^{KDPG} = 36 \pm 5\ M^{-1}\ s^{-1}$), which occurs as a result of a 140-fold decrease in k_{cat} ($k_{cat}^{KDPG} = 0.6 \pm 0.04\ s^{-1}$) and a 170-fold increase in K_M ($K_M^{KDPG} = 17 \pm 3$ mM) (unpublished data). These observations suggest that R49 makes contacts with the substrate or an important negatively charged intermediate, such as the enamine/carbanion, that enhance ligand affinity and catalytic reactivity.

Information-Guided Library Screening. Previously, we concluded that the intracellular concentration of targeted aldol products was likely in the nanomolar to micromolar range, far lower than the K_M value of the wild-type enzyme for these substrates.[15] Therefore, random mutagenesis coupled to in vivo selection identified mutations that lowered the value of K_M but did not improve k_{cat}. Albery and Knowles[38] suggest that the first mutations in the evolution of a new activity often result in "uniform binding" where a mutation has a similar stabilizing effect on both the ground and transition states of the rate-limiting step, leaving the value of k_{cat} unchanged. Many types of interactions, both near and far from the active site, can produce uniform binding enhancements (electrostatic effects, hydrogen bonding, hydrophobic interactions, etc.).[38] Furthermore, these mutations may be dominant when the substrate concentration is significantly lower than the value of K_M. To increase the likelihood of identifying mutations that improve the value of k_{cat}, we expressed KDPG aldolase in the periplasm where the concentration of aldol substrate will more closely reflect the millimolar concentration of the substrate added to the media. This method was particularly successful for identification of the T161S mutation that increased the value of k_{cat} for *S*-KHPB cleavage. For the KHO selections, the identified mutations had little or no effect on the value of k_{cat}, likely resulting from the concentration of KHO (2.5 mM) in the medium being lower than the wild-type K_M value. These data suggest that selection methods using periplasmic expression may be a useful strategy for increasing the odds of finding mutants with higher turnover numbers, an important parameter for biocatalytic applications.

The successful engineering of KDPG aldolase substrate selectivity demonstrates that mutagenesis efforts focused on active site residues can have a profound impact on the specificity and reactivity of an enzyme. While whole gene directed evolution experiments are extremely useful for improving the thermal and chemical stability of enzymes,[39] employing a similar strategy to alter the specificity of aldolase/transaldolase genes has generally led to only modest improvements (6−80-fold) in substrate selectivity and reactivity.[13,15,16,40−43] Additionally, the optimized mutant enzymes often possess improved k_{cat}/K_M and K_M values but lower catalytic turnover numbers. In contrast, efforts combining structural information and site specific saturation mutagenesis have led to large alterations in the enzymatic properties of various aldolase/transaldolases with minimal mutagenesis.[8,11,44−47] In a recent example, Schneider and colleagues[46] used site saturation mutagenesis to identify a single-amino acid substitution in *E. coli* TalB transaldolase that improves the aldol cleavage reaction by 70-fold compared to that of the wild-type. In another example, Royer et al.[47] employed active site-directed mutagenesis to create two variants of *Sulfolobus solfataricus* 2-keto-3-deoxygluconate aldolase that improve the enantioselectivity of the enzyme, preferentially catalyzing the formation of either D-2-keto-3-deoxygluconate or D-2-keto-3-deoxygalactonate

substrate. However, in both examples, the enhanced properties are obtained at a significant cost to the overall catalytic efficiency and turnover number of the mutant when compared to the natural reaction catalyzed by each enzyme. These examples illustrate the power of information-guided evolution approaches to alter the catalytic characteristics of an enzyme with minimal screening effort. Our results add to a growing body of evidence arguing that the targeting of active sites is a highly efficient method for obtaining large enhancements in catalytic activity and substrate selectivity. Remarkably, in this case, the catalytic characteristics of the engineered enzyme match or exceed that of the wild-type enzyme reacting with the natural substrate in terms of efficiency, maximal turnover number, and stereospecificity.

CONCLUSIONS

The development of novel biocatalysts requires balancing many parameters. The engineered enzymes should have high catalytic activity and fidelity for the chemical reaction (including stereochemistry) yet also possess broad substrate tolerance and high protein stability. Frequently, when the substrate tolerance of an enzyme is broadened, the reactivity, fidelity, and stereoselectivity are compromised. Here we have used structure-guided active site mutagenesis to engineer an aldolase that shows significant tolerance for unnatural electrophilic substrates yet retains near wild-type activity. Impressively, this enzyme also maintains exquisite stereoselectivity in the aldol product. This enzyme should prove useful for the synthesis of nikkomycins and other important natural products. Our study highlights the substantial benefit that minor remodeling of the active site architecture can have on substrate specificity and suggests that structure-guided mutagenesis coupled with biochemical analysis and selection techniques provide a useful avenue for effective protein engineering.

ASSOCIATED CONTENT

Supporting Information

Pharmaceutical targets that could be partially synthesized by enzyme-catalyzed aldol condensations (Figure S1), the structure of *E. coli* KDPG aldolase to explain the low activity of the *galacto* sugar (Figure S2), the structure of *E. coli* KDPGal aldolase to explain the stereoselectivity of this enzyme (Figure S3), a list of synthetically useful aldolases (Table S1), and a list of the number of mutants selected in this study (Table S2). This material is available free of charge via the Internet at http://pubs.acs.org.

AUTHOR INFORMATION

Corresponding Author

*Phone: (734) 936-2678. Fax: (734) 647-4865. E-mail: fierke@umich.edu.

Funding

This work was supported by National Institutes of Health Grant GM61596. M.C. received support from Chemical Biology Interface Training Program GM08597.

Notes

The authors declare no competing financial interest.

ACKNOWLEDGMENTS

We thank Matthew J. Walters for providing KDPGal and *R*-KHPB and Lance W. Rider for measuring the kinetic parameters of the R49A KDPG aldolase mutant.

ABBREVIATIONS

DHAP, dihydroxyacetone phosphate; DMSO, dimethyl sulfoxide; HEPES, 4-(2-hydroxyethyl)-1-piperazineethanesulfonic acid; KDPG, 2-keto-3-deoxy-6-phosphogluconate; KDPGal, 2-keto-3-deoxy-6-phosphogalactonate; KHO, 2-keto-4-hydroxyoctonoate; LDH, lactate dehydrogenase; NADH, β-nicotinamide adenine dinucleotide; PCA, pyridine carboxaldehyde; *R*-KHPB, (4*R*)-2-keto-4-hydroxy-4-(2′-pyridyl)butyrate; *S*-KHPB, (4*S*)-2-keto-4-hydroxy-4-(2′-pyridyl)butyrate.

ADDITIONAL NOTES

[a] Selectivity ratio = $[(k_{cat}/K_M^{KDPG})/(k_{cat}/K_M^{KHX})]^{wild\text{-}type}/[(k_{cat}/K_M^{KDPG})/(k_{cat}/K_M^{KHX})]^{mutant}$.
[b] Selectivity ratio = $(activity^{aldehyde}/activity^{D\text{-}GAP})^{mutant}/(activity^{aldehyde}/activity^{D\text{-}GAP})^{wild\text{-}type}$.
[c] Stereoselectivity ratio = $[(k_{cat}/K_M^{KDPG})/(k_{cat}/K_M^{KDPGal})]$.
[d] Stereoselectivity ratio = $[(k_{cat}/K_M^{S\text{-}KHPB})/(k_{cat}/K_M^{R\text{-}KHPB})]$.
[e] $\Delta\Delta G^{\ddagger} = -2.303RT \log[(k_{cat}/K_M^{variant\ 1})/(k_{cat}/K_M^{variant\ 2})]$, where T = 298.15 K and R = 1.987 cal K^{-1} mol^{-1}.

REFERENCES

(1) Samland, A. K., and Sprenger, G. A. (2006) Microbial aldolases as C-C bonding enzymes-unknown treasures and new developments. *Appl. Microbiol. Biotechnol. 71*, 253−264.
(2) Fessner, W. D., and Walter, C. (1997) Enzymatic C-C bond formation in asymmetric synthesis. *Top. Curr. Chem. 184*, 97−194.
(3) Bolt, A., Berry, A., and Nelson, A. (2008) Directed evolution of aldolases for exploitation in synthetic organic chemistry. *Arch. Biochem. Biophys. 474*, 318−330.
(4) Faber, K. (2004) *Biotransformations in Organic Chemistry*, 5th ed., Springer, Berlin.
(5) Clapes, P., Fessner, W. D., Sprenger, G. A., and Samland, A. K. (2010) Recent progress in stereoselective synthesis with aldolases. *Curr. Opin. Chem. Biol. 14*, 154−167.
(6) Sugiyama, M., Hong, Z., Greenberg, W. A., and Wong, C. H. (2007) In vivo selection for the directed evolution of L-rhamnulose aldolase from L-rhamnulose-1-phosphate aldolase (RhaD). *Bioorg. Med. Chem. 15*, 5905−5911.
(7) Schurmann, M., and Sprenger, G. A. (2001) Fructose-6-phosphate aldolase is a novel class I aldolase from *Escherichia coli* and is related to a novel group of bacterial transaldolases. *J. Biol. Chem. 276*, 11055−11061.
(8) Schneider, S., Gutierrez, M., Sandalova, T., Schneider, G., Clapes, P., Sprenger, G. A., and Samland, A. K. (2010) Redesigning the active site of transaldolase TalB from *Escherichia coli*: New variants with improved affinity towards nonphosphorylated substrates. *ChemBioChem 11*, 681−690.
(9) Garrabou, X., Joglar, J., Parella, T., Crehuet, R., Bujons, J., and Clapes, P. (2011) Redesign of the phosphate binding site of L-rhamnulose-1-phosphate aldolase towards a dihydroxyacetone dependent aldolase. *Adv. Synth. Catal. 353*, 89−99.
(10) Shelton, M. C., Cotterill, I. C., Novak, S. T., Poonawala, R. M., Sudarshan, S., and Toone, E. J. (1996) 2-keto-3-deoxy-6-phosphogluconate aldolases as catalysts for stereocontrolled carbon-carbon bond formation. *J. Am. Chem. Soc. 118*, 2117−2125.
(11) Baker, P., Carere, J., and Seah, S. Y. (2011) Probing the molecular basis of substrate specificity, stereospecificity, and catalysis in the class II pyruvate aldolase, BphI. *Biochemistry 50*, 3559−3569.
(12) Wang, W., Baker, P., and Seah, S. Y. (2010) Comparison of two metal-dependent pyruvate aldolases related by convergent evolution: Substrate specificity, kinetic mechanism, and substrate channeling. *Biochemistry 49*, 3774−3782.
(13) Fong, S., Machajewski, T. D., Mak, C. C., and Wong, C. H. (2000) Directed evolution of D-2-keto-3-deoxy-6-phosphogluconate aldolase to new variants for the efficient synthesis of D- and L-sugars. *Chem. Biol. 7*, 873−883.

(14) Wymer, N., Buchanan, L. V., Henderson, D., Mehta, N., Botting, C. H., Pocivavsek, L., Fierke, C. A., Toone, E. J., and Naismith, J. H. (2001) Directed evolution of a new catalytic site in 2-keto-3-deoxy-6-phosphogluconate aldolase from *Escherichia coli*. *Structure 9*, 1−9.
(15) Cheriyan, M., Walters, M. J., Kang, B. D., Anzaldi, L. L., Toone, E. J., and Fierke, C. A. (2011) Directed evolution of a pyruvate aldolase to recognize a long chain acyl substrate. *Bioorg. Med. Chem. 19*, 6447−6453.
(16) Ran, N., and Frost, J. W. (2007) Directed evolution of 2-keto-3-deoxy-6-phosphogalactonate aldolase to replace 3-deoxy-D-arabino-heptulosonic acid 7-phosphate synthase. *J. Am. Chem. Soc. 129*, 6130−6139.
(17) Stock, S. D., Hama, H., Radding, J. A., Young, D. A., and Takemoto, J. Y. (2000) Syringomycin E inhibition of *Saccharomyces cerevisiae*: Requirement for biosynthesis of sphingolipids with very-long-chain fatty acids and mannose- and phosphoinositol-containing head groups. *Antimicrob. Agents Chemother. 44*, 1174−1180.
(18) Luesch, H., Yoshida, W. Y., Moore, R. E., and Paul, V. J. (2000) Isolation and structure of the cytotoxin lyngbyabellin B and absolute configuration of lyngbyapeptin A from the marine cyanobacterium *Lyngbya majuscula*. *J. Nat. Prod. 63*, 1437−1439.
(19) Schlüter, U. (1982) Ultrastructural evidence for inhibition of chitin synthesis by nikkomycin. *Dev. Genes Evol. 91*, 205−207.
(20) Henderson, D. P., Shelton, M. C., Cotterill, I. C., and Toone, E. J. (1997) Stereospecific preparation of the N-terminal amino acid moiety of nikkomycins Kx and Kz via a multiple enzyme synthesis. *J. Org. Chem. 62*, 7910−7911.
(21) Ling, H., Wang, G., Tian, Y., Liu, G., and Tan, H. (2007) SanM catalyzes the formation of 4-pyridyl-2-oxo-4-hydroxyisovalerate in nikkomycin biosynthesis by interacting with SanN. *Biochem. Biophys. Res. Commun. 361*, 196−201.
(22) Griffiths, J. S., Cheriyan, M., Corbell, J. B., Pocivavsek, L., Fierke, C. A., and Toone, E. J. (2004) A bacterial selection for the directed evolution of pyruvate aldolases. *Bioorg. Med. Chem. 12*, 4067−4074.
(23) Zheng, L., Baumann, U., and Reymond, J. L. (2004) An efficient one-step site-directed and site-saturation mutagenesis protocol. *Nucleic Acids Res. 32*, e115.
(24) Ponce, E., Flores, N., Martinez, A., Valle, F., and Bolivar, F. (1995) Cloning of the two pyruvate kinase isoenzyme structural genes from *Escherichia coli*: The relative roles of these enzymes in pyruvate biosynthesis. *J. Bacteriol. 177*, 5719−5722.
(25) Buchanan, L. V., Mehta, N., Pocivavsek, L., Niranjanakumari, S., Toone, E. J., and Naismith, J. H. (1999) Initiating a structural study of 2-keto-3-deoxy-6-phosphogluconate aldolase from *Escherichia coli*. *Acta Crystallogr. D55*, 1946−1948.
(26) Cheriyan, M., Toone, E. J., and Fierke, C. A. (2007) Mutagenesis of the phosphate binding pocket of KDPG aldolase enhances selectivity for hydrophobic substrates. *Protein Sci. 16*, 2368−2377.
(27) Sambrook, J., and Russell, D. W. (2001) *Molecular Cloning: A Laboratory Manual*, Vol. 3, 3rd ed., Cold Spring Harbor Laboratory Press, Plainview, NY.
(28) Walters, M. J., Srikannathasan, V., McEwan, A. R., Naismith, J. H., Fierke, C. A., and Toone, E. J. (2008) Characterization and crystal structure of *Escherichia coli* KDPGal aldolase. *Bioorg. Med. Chem. 16*, 710−720.
(29) Allard, J., Grochulski, P., and Sygusch, J. (2001) Covalent intermediate trapped in 2-keto-3-deoxy-6-phosphogluconate (KDPG) aldolase structure at 1.95-angstrom resolution. *Proc. Natl. Acad. Sci. U.S.A. 98*, 3679−3684.
(30) Fullerton, S. W. B., Griffiths, J. S., Merkel, A. B., Cheriyan, M., Wymer, N. J., Hutchins, M. J., Fierke, C. A., Toone, E. J., and Naismith, J. H. (2006) Mechanism of the class I KDPG aldolase. *Bioorg. Med. Chem. 14*, 3002−3010.
(31) Rapoza, M. P., and Webster, R. E. (1993) The filamentous bacteriophage assembly proteins require the bacterial SecA protein for correct localization to the membrane. *J. Bacteriol. 175*, 1856−1859.
(32) Hutchison, C. A., Nordeen, S. K., Vogt, K., and Edgell, M. H. (1986) A complete library of point substitution mutations in the glucocorticoid response element of mouse mammary tumor virus. *Proc. Natl. Acad. Sci. U.S.A. 83*, 710−714.
(33) Heine, A., Luz, J. G., Wong, C. H., and Wilson, I. A. (2004) Analysis of the class I aldolase binding site architecture based on the crystal structure of 2-deoxyribose-5-phosphate aldolase at 0.99 Å resolution. *J. Mol. Biol. 343*, 1019−1034.
(34) Jia, J., Schorken, U., Lindqvist, Y., Sprenger, G. A., and Schneider, G. (1997) Crystal structure of the reduced Schiff-base intermediate complex of transaldolase B from *Escherichia coli*: Mechanistic implications for class I aldolases. *Protein Sci. 6*, 119−124.
(35) LowKam, C., Liotard, B., and Sygusch, J. (2010) Structure of a class I tagatose-1,6-bisphosphate aldolase: Investigation into an apparent loss of stereospecificity. *J. Biol. Chem. 285*, 21143−21152.
(36) St-Jean, M., Lafrance-Vanasse, J., Liotard, B., and Sygusch, J. (2005) High resolution reaction intermediates of rabbit muscle fructose-1,6-bisphosphate aldolase: Substrate cleavage and induced fit. *J. Biol. Chem. 280*, 27262−27270.
(37) Radaev, S., Dastidar, P., Patel, M., Woodard, R. W., and Gatti, D. L. (2000) Structure and mechanism of 3-deoxy-D-manno-octulosonate 8-phosphate synthase. *J. Biol. Chem. 275*, 9476−9484.
(38) Albery, W. J., and Knowles, J. R. (1976) Evolution of enzyme function and the development of catalytic efficiency. *Biochemistry 15*, 5631−5640.
(39) O'Fagain, C. (2011) Engineering protein stability. *Methods Mol. Biol. 681*, 103−136.
(40) DeSantis, G., Liu, J., Clark, D. P., Heine, A., Wilson, I. A., and Wong, C. H. (2003) Structure-based mutagenesis approaches toward expanding the substrate specificity of D-2-deoxyribose-5-phosphate aldolase. *Bioorg. Med. Chem. 11*, 43−52.
(41) Hsu, C. C., Hong, Z., Wada, M., Franke, D., and Wong, C. H. (2005) Directed evolution of D-sialic acid aldolase to L-3-deoxy-manno-2-octulosonic acid (L-KDO) aldolase. *Proc. Natl. Acad. Sci. U.S.A. 102*, 9122−9126.
(42) Jennewein, S., Schurmann, M., Wolberg, M., Hilker, I., Luiten, R., Wubbolts, M., and Mink, D. (2006) Directed evolution of an industrial biocatalyst: 2-Deoxy-D-ribose 5-phosphate aldolase. *Biotechnol. J. 1*, 537−548.
(43) Williams, G. J., Domann, S., Nelson, A., and Berry, A. (2003) Modifying the stereochemistry of an enzyme-catalyzed reaction by directed evolution. *Proc. Natl. Acad. Sci. U.S.A. 100*, 3143−3148.
(44) Williams, G. J., Woodhall, T., Nelson, A., and Berry, A. (2005) Structure-guided saturation mutagenesis of N-acetylneuraminic acid lyase for the synthesis of sialic acid mimetics. *Protein Eng., Des. Sel. 18*, 239−246.
(45) Toscano, M. D., Muller, M. M., and Hilvert, D. (2007) Enhancing activity and controlling stereoselectivity in a designed PLP-dependent aldolase. *Angew. Chem., Int. Ed. 46*, 4468−4470.
(46) Schneider, S., Sandalova, T., Schneider, G., Sprenger, G. A., and Samland, A. K. (2008) Replacement of a phenylalanine by a tyrosine in the active site confers fructose-6-phosphate aldolase activity to the transaldolase of *Escherichia coli* and human origin. *J. Biol. Chem. 283*, 30064−30072.
(47) Royer, S. F., Haslett, L., Crennell, S. J., Hough, D. W., Danson, M. J., and Bull, S. D. (2010) Structurally informed site-directed mutagenesis of a stereochemically promiscuous aldolase to afford stereochemically complementary biocatalysts. *J. Am. Chem. Soc. 132*, 11753−11758.
(48) Cotterill, I. C., Shelton, M. C., Machemer, D. E., Henderson, D. P., and Toone, E. J. (1998) Effect of phosphorylation on the rate of unnatural electrophiles with KDPG aldolase. *J. Chem. Soc., Perkin Trans. 1*, 1335−1341.